GE Energy

David H. Hinds
Manager, ESBWR

PO Box 780 M/C L60
Wilmington, NC 28402-0780
USA

T 910 675 6363
F 910 362 6363
david.hinds@ge.com

MFN 06-268

Docket No. 52-010

August 12, 2006

U.S. Nuclear Regulatory Commission
Document Control Desk
Washington, D.C. 20555-0001

Subject: **Response to Portion of NRC Request for Additional Information Letter No. 43 Related to ESBWR Design Certification Application – ESBWR Containment Design and Probabilistic Risk Assessment Re: Containment Fragility Analysis – (Release A) RAI Numbers 6.2-95, 6.2-97, 19.2-41, 19.2-44 to 19.2-46, 19.2-49, 19.2-50 and 19.2-57**

Enclosure 1 contains GE's responses and Enclosure 2 the DCD markup pages to the subject NRC RAIs transmitted via the Reference 1 letter.

If you have any questions about the information provided here, please let me know.

Sincerely,

George Stramboe
for

David H. Hinds
Manager, ESBWR

D068

Reference:

1. MFN 06-237, Letter from U.S. Nuclear Regulatory Commission to David Hinds, *Request for Additional Information Letter No. 43 Related to ESBWR Design Certification Application,* July 18, 2006

Enclosure:

1. MFN 06-268 – Partial Response to NRC RAIs 6.2 and 19.2 Release A RAI 6.2-95, -97, 19.2-41, -44, -45, -46, -49, -50 and –57
2. MFN 06-268 – DCD Section 6.2 and NEDO 33201 Table B.8-1 Markup Pages for RAIs 6.2-95, & -97, and RAI 19.2-45c

cc:

WD Beckner	USNRC (w/o enclosures)
AE Cubbage	USNRC (with enclosures)
LA Dudes	USNRC (w/o enclosures)
GB Stramback	GE/San Jose (with enclosures)
eDRF	0000-0056-7509

Enclosure 1

MFN 06-268

Partial Response to NRC RAIs 6.2 and 19.2 Release A
RAI 6.2-95, -97. 19.2-41, -44,-45, -46, -49, -50 and -57

NRC RAI 6.2-95

In DCD Tier 2, 6.2.5.4, for the concrete containment, the statement is made: "The analysis results show that when the internal pressure reaches as high as 1.468 MPa, the maximum liner strain is only 0.165% tension, which is well within the 0.3% limit for Factored Load Category specified in ASME Table CC-3720-1." Provide the following additional information in the DCD:

a) Comparison of the concrete and rebar stresses to their factored load allowables.

b) Of the liner, concrete, and rebar, which limits the Level C pressure capability of the concrete containment (ignoring the steel penetrations)?

c) Compare the rebar strains to the liner strains at the 1.468 MPa load level. Explain any significant differences between the two.

d) The spacing between the anchors for the liner plate, including drawings to show how the liner is anchored into the concrete.

e) Locations (typical) of the heat affected zone at the liner weld seams and the proximity to liner anchors.

GE Response

a) The pressure value of 1.468 MPa is a pressure at which a concrete section loses its capability to resist shear. It is conservatively assumed that shear reinforcement does not participate to resist shear when the concrete element cracks. This pressure value is taken as the ultimate pressure capacity of the concrete containment. This occurs at the connection of SP slab to the RCCV wall. At this pressure, the concrete compression is 31.1 MPa which is less than f'c (34.5 MPa) but is higher than the allowable of 0.75f'c for the Factored Loads, the rebar stress is 418.63 MPa which is less than the allowable rebar stress under Factored Loads, and the liner strain is 0.165% which is well within the 0.3% limit for Factored Load Category.

The pressure value of 1.41 MPa is a pressure at which the concrete compression reaches 23.83 MPa which is very close to 0.75f'c = 25.9 MPa, the allowable compressive stress for Factored Loads. At this pressure, the rebar stress is 417.63 MPa for radial bars at connection of Diaphragm Floor to the RCCV wall.

The concrete stresses under 1.468 MPa, ultimate pressure and 1.41 MPa, the pressure that concrete compression is slightly lower that the allowable concrete compression for Factored Loads, are summarized and compared with the allowable concrete compression for Factored Loads as shown in Table 6.2-95(1). Similarly, the rebar stresses in the RCCV under these two pressure loads are summarized and compared in Table 6.2-95(2).

Concrete		
allowable compressive stress for Factored Loads	under 1.468 MPa (Ultimate pressure) (stress at joint of SP slab/WW)	under 1.410 MPa pressure (i) (same location)
0.75 f'c = 25.9 MPa	31.1 MPa	23.83 MPa

Note: (i) Pressure for which concrete compression is slightly lower than the allowable concrete compression for Factored Loads.

Table 6.2-95(1). Comparison of concrete stresses and the allowable for Factored Load

Rebars		
allowable stress for Factored Loads (ii)	under 1.468 MPa (Ultimate pressure) Stress at joint of DF and RCCV wall	under 1.410 MPa pressure (ii) (same location)
$f_{2\varepsilon y}$ = 420.29 MPa	418.63 MPa	417.63 MPa

Note: (ii) Yield strength taken at $2\varepsilon_y$ according to ASME CC-3422(e).

Table 6.2-95(2). Comparison of rebar stresses and the allowable for Factored Load

b) For Factored Loads Category, (Equivalent to Level C), the allowable for concrete compression stress is 0.75f'c = 25.9 MPa. For a pressure of 1.410 MPa, the compression stress in concrete is 23.83 MPa. This pressure (1.410 MPa) is conservatively limiting the level C of concrete, rebar and liner. It should be noted that demonstration of Level C structural integrity for concrete containments as required by RG 1.7 Revision 3 is to meet CC-3720 requirements which are for liners only. Meeting factored load allowables for concrete and rebar is not a requirement for Level C pressure capability of concrete containments.

c) Figures 6.2-95(2), (3) and (4) show a comparison of the liner strains and rebar strains for concrete elements in contact with the liner in the radial, meridian and hoop directions, respectively, along the nodes shown in Figure 6.2-95(1). There are no significant differences between them if the rebars belong to a plane parallel to that of the liner. The comparison of the vertical shear rebar strains to the vertical liner strains (mat, SP slab or Top Slab), as well as of the radial shear rebar strains to the radial liner strains (Pedestal, Wetwell or Drywell) shows some differences. The explanation lies in how the load is being resisted, mainly, by bending and shear of

those structural elements. The shear stress distribution in shear rebars is therefore slightly different from that of the liner

Accordingly, the liner is mostly compressed in those areas, whereas the rebars can be under tensile or compression stress.

Other effects such as the proximity to the joint between structural members, as well as the presence of slabs, cause additional local differences. Note that, in spite of the differences, all rebar and liner strains are of the same order.

As for the hoop strain comparison, since none of the previous factors are present, liner and rebar deform in a consistent manner, such that there are not significant differences between them.

d) Figure 3G.1-48 and 49 of DCD Appendix G show the liner anchor configuration and how the liner is anchored to the concrete.

e) Scallops are prepared in the liner anchors to avoid interference with liner weld seams. More than 25mm (about 1 inch) clearance for both sides of weld seams is considered for this purpose. Figure 6.2-95(5) shows the typical scallop configuration of liner anchor

DCD Section 6.2.5.4.2 will be revised in the next update as noted in the attached markups.

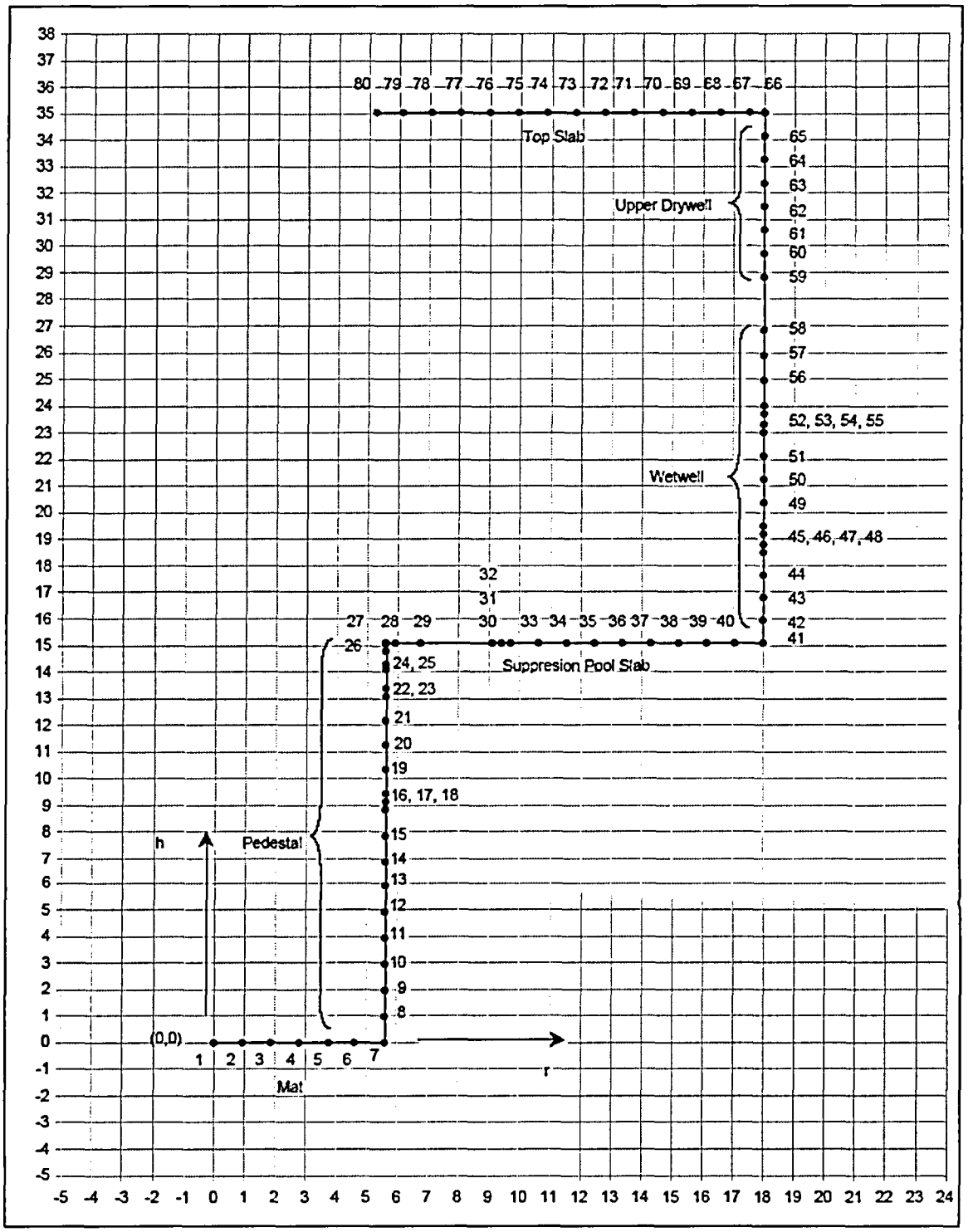

Figure 6.2-95(1). Nodal Locations

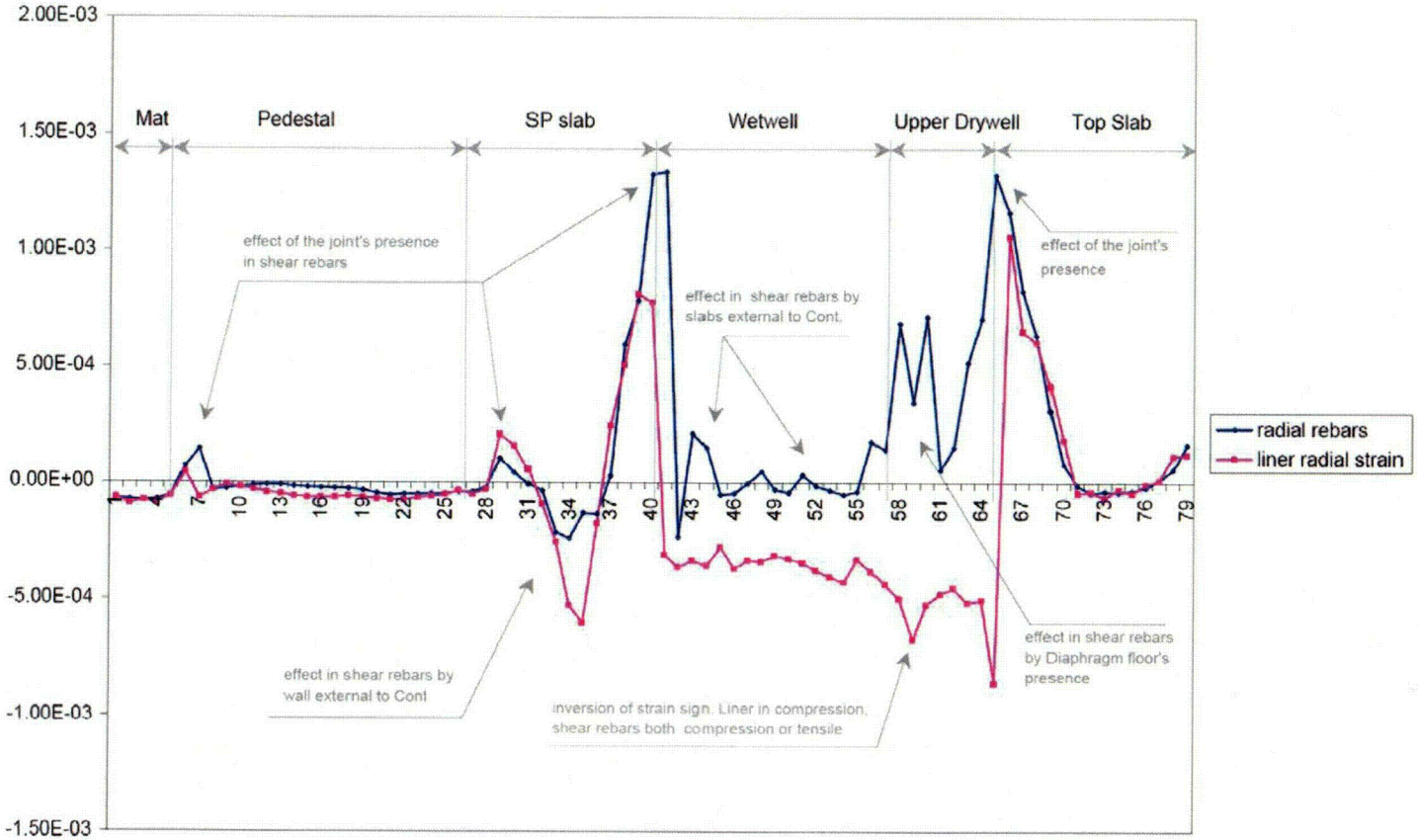

Figure 6.2-95(2). Radial liner strain and Radial rebar strain
Position of points in horizontal axis are shown in Figure 6.2-95(1)

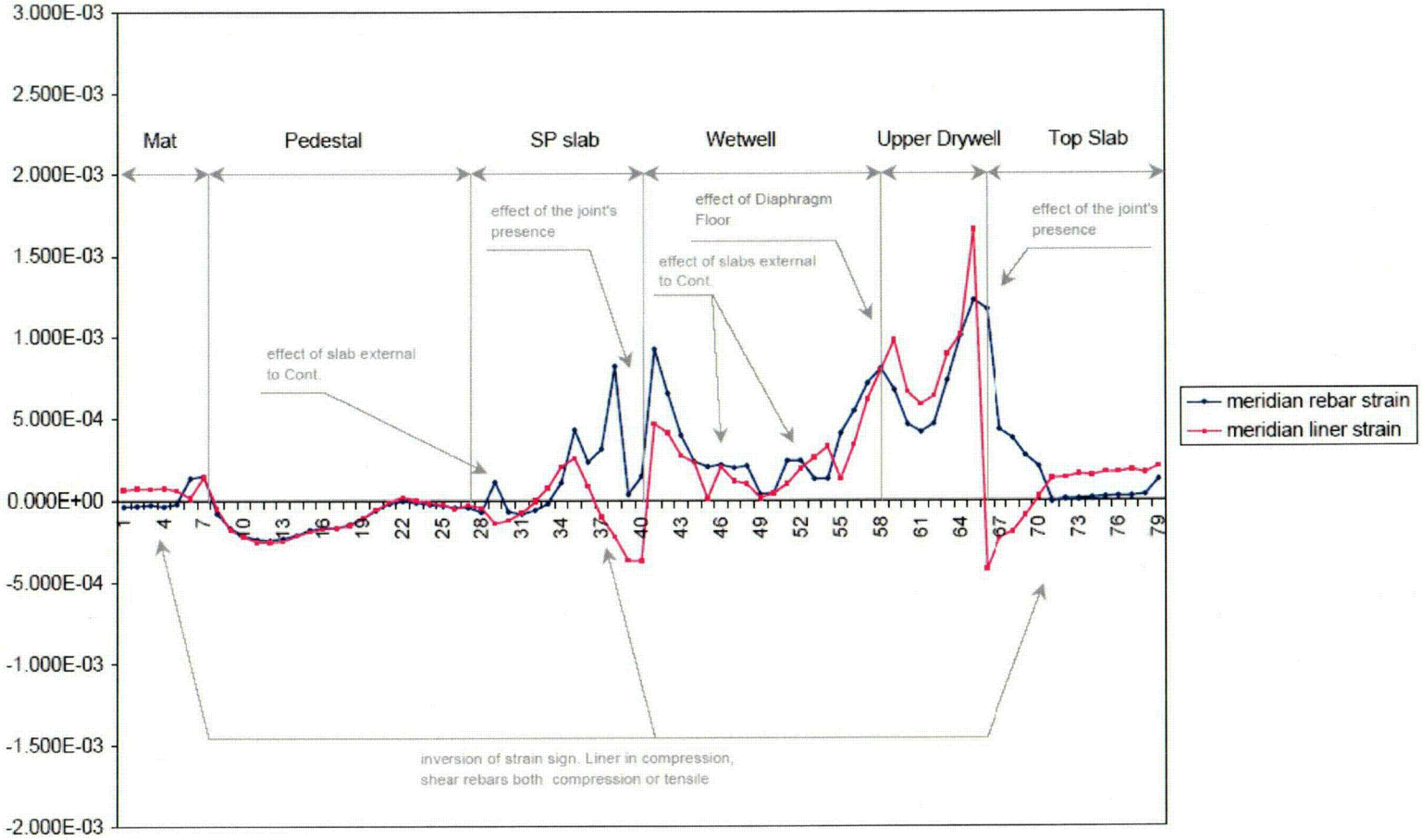

Figure 6.2-95(3). Meridian liner strain and meridian rebar strain
Position of points in horizontal axis are shown in Figure 6.2-95(1)

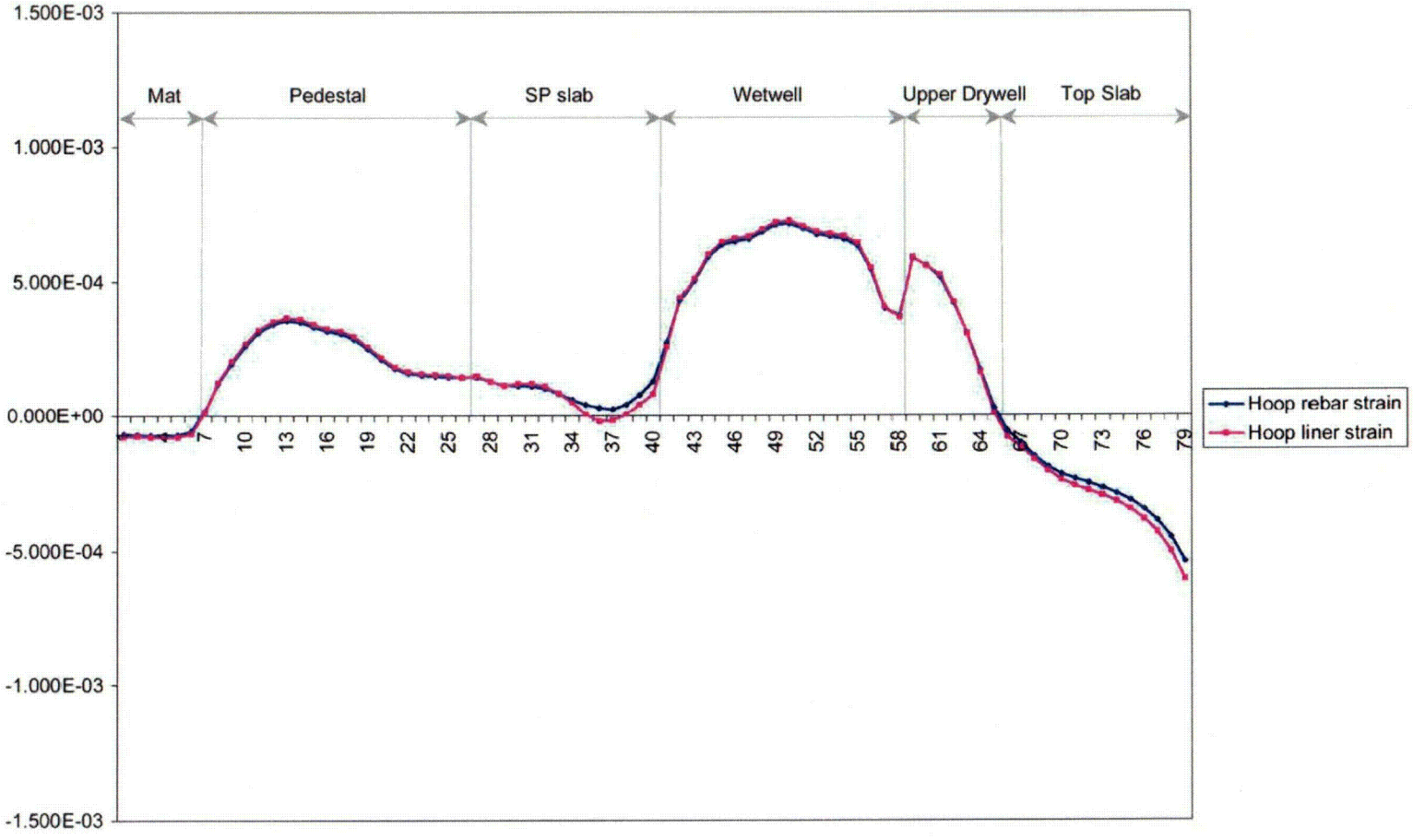

Figure 6.2-95(4). Hoop liner strain and hoop rebar strain
Position of points in horizontal axis are shown in Figure 6.2-95(1)

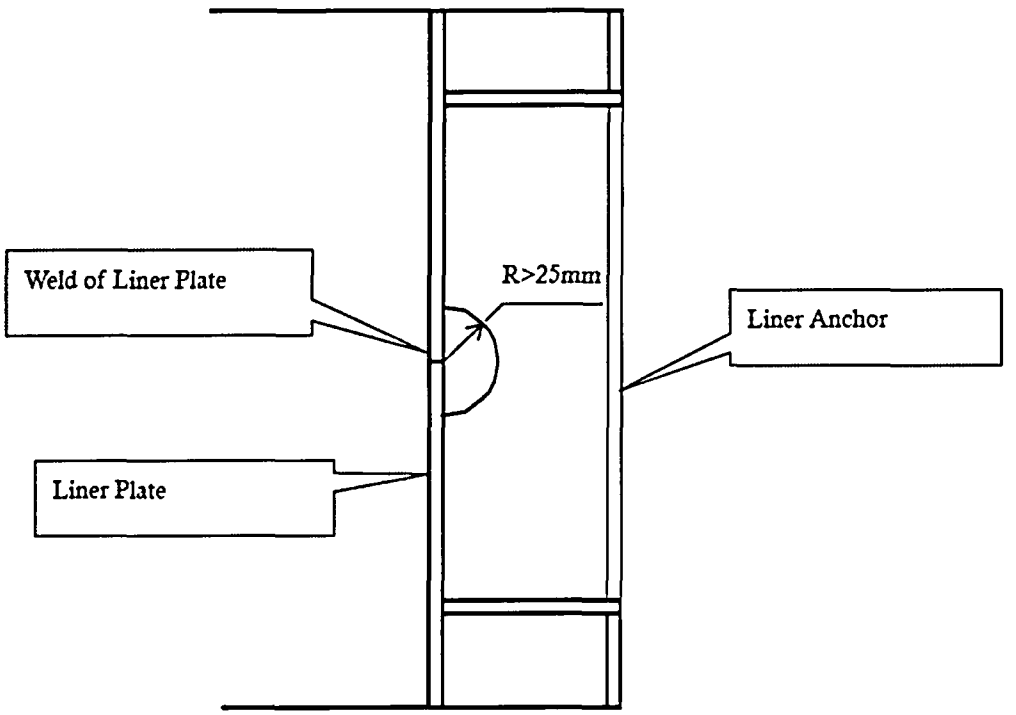

Figure 6.2-95(5). Typical Scallop Configuration of Liner Anchor

NRC RAI 6.2-97

In DCD Tier 2, 6.2.5.4, for other steel penetrations, the statement is made: "The Level C pressure capabilities of the steel components of major penetrations are summarized in Table 6.2-46. The governing pressure is 1.182 MPa, which is controlled by the buckling strength of the drywell head." Include in the DCD a description of the calculations performed to predict the Level C pressure capability for the other steel penetrations.

GE Response

The most critical of the other RCCV steel penetrations are the main steam pipe penetrations. They have the biggest flued head and anchor sleeves.

Considering the loads transmitted by the main steam pipes, the maximum Level C pressure capability can be up to 3.377 MPa.

Concerning the other steel penetrations, they have higher Level C pressure capability.

DCD Section 6.2.5.4.2 and Table 6.2-46 will be revised in the next update as noted in the attached markup.

NRC RAI 19.2-41

In DCD Tier 2, 19.2.4, GE only provides a reference to the GE Probabilistic Risk Assessment (PRA) report. The detailed fragility analysis for containment ultimate strength is contained in the GE PRA report, Revision 1, Appendix B.8. It is unclear how the 10 CFR Part 50.44(c)(5) requirement is addressed. It is also unclear how the SECY 93-087 requirement, which requires satisfaction of Service Level C limits, including considerations of structural instability, for the more likely severe accident challenges for approximately 24 hours following the onset of core damage under most likely severe accident challenges, and, following this period the containment should continue to provide a barrier against the uncontrolled release of fission products, is satisfied by the fragility analysis. Provide the following information in ESBWR DCD Tier 2, Section 19.2.4:

a) A summary of the GE PRA report, Revision 1, Appendix B.8, including all pertinent results;

b) A discussion of how the 10 CFR Part 50.44(c)(5) requirement and the SECY 93-087 requirement are satisfied;

c) Available test data of over-pressurization of containment structures similar to the ESWR design (with more geometric discontinuities than typical containments in the current fleet of reactors) at both ambient and severe temperature environments.

GE Response

a) Pertinent information in the GE PRA report, Revision 1, Appendix B.8 will be summarized in DCD Chapter 19 the next DCD revision.

b) The 10 CFR Part 50.44(c)(5) requirement and the SECY 93-087 requirement are satisfied by meeting the ASME Section III acceptance criteria of Service Level C or Factored Load Category stipulated in RG 1.7 Revision 3. Details are documented in DCD Section 6.2.5.4.2.

c) Available test data of over-pressurization of containment structures relevant to ESBWR reinforced concrete containment vessel (RCCV) are two tests conducted by Sandia National Laboratories: a reinforced containment 1/6th scale test conducted in the late eighties and the more recent ¼ scale test of a pre-stressed containment. However, in order to appropriately interpret the results of these two tests relative to ESBWR, we must know the limitations on our abilities to simulate experimentally the failure behavior of concrete containments.

Concrete containment failure mode under internal pressure is critically dependent on the pressurization medium, gas or water. The most likely failure mode for concrete containments, whether reinforced or pre-stressed, tested under water

pressurization is burst, while gas pressurization would produce only leakage. This has to do with the balance between the rate of pressurization and the rate of depressurization at the instant of failure initiation by liner cracking or other venting mechanisms. Under water pressurization, a tiny change in the volume of the nearly incompressible fluid requires a huge pressure increment, whereas for gas pressurization the opposite is true. This implies that the pumping rate of the pressurization medium at the instant of failure initiation governs the failure mode. Behavioral differences between the reinforced and pre-stressed structures, namely, ductile behavior for the former and brittle behavior for the latter, can alter the failure mode if the pressurization medium is changed. For example, a pre-stressed containment could fail in a ductile manner, i.e. in a leak-before-break mode, under gas pressure. Therefore, one should be careful in using the test results directly to predict containment behavior under over-pressurization.

The experimental evidence shows that the failure mode for reinforced concrete containments internally pressurized by gas (air or nitrogen) is by leakage through liner cracks at points of discontinuity such as at stud locations, insert plates or thickened flanges around penetration covers. The Sandia 6th Scale reinforced concrete model confirmed this behavior. The leakage pressure for that test was 145 psig, which is 3.22 times design pressure. At 145 psig, the model could not be pressurized further, and for reasons mentioned above the pressurization rate could not keep up with the leakage rate. On the other hand, Sandia's 1/4th scale model of a pre-stressed concrete containment failed catastrophically at 3.6 times the design pressure. In this case, the rupture of the hoop tendons caused very sudden loss of structural stiffness, which overwhelmed the ability of the liner to form fuse-like pressure relief mechanism. The question is: if the pressurization medium were air instead of water, would the failure have been a catastrophic burst? Most likely it would be a leakage type failure, despite the brittle nature of the structure, but of a different, perhaps somewhat larger, configuration than in reinforced concrete. It should be noted parenthetically that the 3.6-factor was predicted using simple hand calculations. The leak-before-break failure mode could not be demonstrated in large-scale models because of the very large air volume required.

The robust design of the concrete pressure boundary of ESBWR is expected to perform significantly better than the Sandia 1/6th scale model, even considering its geometric discontinuities. However, treating the 1/6th scale model as a guide for judging the ultimate pressure capacity of ESBWR's concrete pressure boundary, we can use the global strain as an indicator. An axi-symmetric global analysis of the Sandia model, and the measured far field liner strains, gave a value of about 1.1% at ultimate pressure for a mid-height location, about the same elevation as the failure location in the insert plate (see Figure 5.3.6 in NUREG/CR 5341, SAND89-0349, dated October 1989). Clearly, the failure strain in the insert plate must have been several times this value due to strain concentration at the discontinuity. If we were to assume that a similar far field strain value would cause failure in the ESBWR liner at a point of discontinuity,

we would conclude that for the ESBWR to develop failure in its concrete pressure boundary, the global analysis must show a far field strain value of at least 1%. As shown in Table B.8-1 of the PRA report, the maximum liner strain calculated by ANSYS nonlinear analysis is only 0.165% which is well within the code allowable when the internal pressure is as high as 1.468 MPa (4.7 times design pressure). Such a large margin should easily compensate for the lack of data at high temperature.

The above discussion indicates that the ESBWR containment ultimate pressure capacity would not be controlled by the concrete strength. The steel drywell head is the weak link as concluded in Appendix B.8 of the PRA report.

No DCD changes will be made in response to this RAI.

NRC RAI 19.2-44

In PRA Revision 1, Appendix B.8.1, GE provides the reinforced concrete containment vessel (RCCV) nonlinear analysis using an ANSYS axisymmetric reinforced concrete model. The analysis result from the ANSYS model was used to determine the containment ultimate pressure strength at ambient temperature. Since ANSYS uses the smeared material model for reinforced concrete, certain subjective inputs are required such as tension stiffening and shear retention when concrete cracks, material properties and failure criteria. Discuss the ANSYS model, including:

a) the GE selection of the parameters for tension stiffening and shear retention in the model and the bases for the selection;

b) the adequacy of the mesh refinement to capture local stress/strain concentrations in regions where geometry changes sharply, such as the corners between top slab/upper dry well (UDW) wall, wet well (WW) wall/suppression pool (SP) floor, SP floor/pedestal, pedestal/basemat;

c) the validation of the ANSYS reinforced concrete material model against other known commercial codes, such as ANACAP or ABAQUS, etc., on similar structures and loading, and their analysis comparisons;

d) a clarification of the last statement in Appendix B.8.1.3 "The strength of the non-axisymmetric top slab region is evaluated by extrapolation of the elastic analysis results using a 3D finite element model," since the RCCV analysis GE used is based on a nonlinear ANSYS model;

e) input material properties (including stress-strain relations up to failures) applied in the ANSYS model for concrete, rebars and liners. Explain how the strain hardening behavior of mild steel used for rebars is modeled in ANSYS;

f) a description of how the liner is connected to concrete elements in the ANSYS model;

g) how the non-axisymmetric Gravity-Driven Cooling System (GDCS) pool structures are considered in the ANSYS axisymmetric model/analysis. Was the weight (structure and water) and an approximation of its stiffness used in the ANSYS model? If yes, explain in detail. If not, provide a detailed technical basis for exclusion.

h) a detailed explanation regarding the importance of modeling the soil below the foundation mat. The extent of the foundation in the ANSYS model is only a piece of the much larger foundation mat supporting the containment, reactor building, and fuel building. If coupling to the soil is important for this analysis, justify why it is not necessary to include the entire foundation with representation of the other stiffness characteristics of the building.

i) a detailed explanation regarding the statement in Appendix B.8.1.2 "The [ANSYS] program utilizes a stepwise linear iteration technique." Are both

material and geometric non-linearity effects considered in the ANSYS analysis? What numerical technique is used to establish convergence (e.g., modified Newton-Raphson) at each load step? What is the convergence criterion applied to ensure satisfaction of the nonlinear equilibrium equations at each load step? What is the convergence criterion applied to ensure satisfaction of the nonlinear equilibrium equations at each load step? Describe the load step/iteration strategy.

GE Response

a) Stress stiffening properties are not taken into account. This feature is not recommended by the ANSYS computer program for concrete non-linear calculations. Regarding the shear retention properties of the model, when cracking occurs in the concrete elements (with cracking and crushing properties), the loss of shear resistance is not transferred to the rebars, which have no shear stiffness. To prevent possible fictitious crushing of the concrete before proper load transfer through a closed crack, the load was applied in small increments.

b) The controlling criterion in the mesh refinement was to represent the hoop and vertical reinforcement layers in the internal and external faces of the containment, as well as the radial shear reinforcement between both layers. According to that strategy, the elements in regions where the geometry changes sharply are between 0.2x0.2m to 0.3x0.3m for walls between 20m high and 2.4m deep. As an example, the junctions at the SP Slab and the RCCV wall or RCCV wall and Top Slab are made up of 25 to 30 brick elements and 72 to 84 nodes. With this level of mesh refinement, stress and deformation in the element nodes are considered sufficiently accurate.

c) A comparison between the ANSYS and ABAQUS computer programs for nonlinear calculations involving reinforced concrete is addressed in the attachment to this RAI.

d) The structure above the top slab is non-axisymmetric. To account for its stiffness in the axisymmetric model, a separate ANSYS 3D shell model was built using the actual geometry of the top slab integrated with the upper pool structure . A unit pressure load was applied upwards from the containment side and the vertical displacement calculated. Young's modulus of the axisymmetric portion representing the pool girders in the axisymmetric model was selected to yield the same vertical displacement under unit pressure as that of the 3D shell model. The density of this portion of the axisymmetric model is established to give the same total mass as the actual geometry.

e) Material properties are shown in Tables 19.2-44(1) and (2). The steel strain hardening behaviours are taken into account using a bilinear strain-stress scheme, with kinematic hardening properties. The hardening rule describes the changing of the yield surface (in stress space) with progressive yielding, so that the

conditions (i.e. stress states) for subsequent yielding can be established. Kinematic hardening assumes that the yield surface remains constant in size and the surface translates in stress space with progressive yielding.

f) In the ANSYS model, the shell element's nodes representing the liner, and the brick element's nodes representing the concrete, go together. Concrete and liner elements share the same nodes.

g) Since the ANSYS model is axisymmetric and the geometry and position of the GDCS Pools is non-axisymmetric, the mass of the pool structure and water was spread on the axisymmetric model on the SP Slab level, and their stiffnesses neglected.

h) The soil underneath the foundation mat was modeled using linear spring constants for soft soil with the objective to maximize bending deformation in the mat. Since containment internal pressure is the only loading of interest in this analysis and the fuel building, located far away from the containment, is not directly loaded, the stiffness of the portion of the mat belonging to the FB is neglected, and only its mass is considered and spread on the axisymmetric model.

i) Material non-linearities are taken into account. Steel properties are included by means of the Young modulus, yield strain, tangent modulus and ultimate strain shaping a bilinear stress-strain scheme. Concrete properties are intended to account for cracking and crushing by means of Drucker-Prager parameters. Geometric non-linearities are also taken into account. Pressure normal to surfaces is following the deformed geometry in each load step. In each load step, the previous deformed geometry is used, but the stiffness matrix is not a function of the displacement as in the case of large deformation calculation. This assumption is considered correct in view of the small ratio of radial deflection to radius that is on the order of 10E-3. ANSYS performs a Newton-Raphson scheme to figure out the convergence of the non-linear equilibrium equations at each load step. The convergence criterion is rearranged for some load steps along the calculation to reach convergence. This strategy is followed until divergence is reached for the controlling failure mode by shear as described in a).

Elements	Steel type	Poisson	Strain		Strength (kN/m^2)
Rebars	ASTM A615 Gr-60	0.3	ε_y	0.005	4.14E+05
			ε_u	0.07	6.21E+05
Carbon steel (liner)	ASME SA-516 Gr-70	0.3	ε_y	0.0013	2.62E+05
			ε_u	0.17 (iii)	4.83E+05
Stainless steel (liner)	ASME SA-240 Type 304L	0.3	ε_y	0.001	1.72E+05
			ε_u	0.40	4.83E+05

Note (iii): 17% ultimate strain in 8". Conservatively lower that 21% elongation in 2". (data from ASME SA-516 Gr-70, Table 2).

Table 19.2-44(1). Material properties. Liner and rebar

Material	f'c (MPa)	Elastic modulus (kN/m^2)	Poisson	Uniaxial Tension (kN/m^2)	Uniaxial Comp. (kN/m^2)	Cohesion(iv) (kN/m^2)	Flow angle(iv)	Fric. angle(iv)
Basemat concrete	27.6	2.79E+07	0.17	1.74E+03	2.76E+04	3.47E+03	30	61.77
Other concrete	34.5	2.79E+07	0.17	1.95E+03	3.45E+04	4.10E+03	30	63.24

Note (iv): Drucker-Prager parameters as a function of Uniaxial tension and Uniaxial compression strengths. Flow angle assumed to be 30°.

Table 19.2-44(2). Material properties. Concrete

No DCD changes will be made in response to this RAI.

NRC RAI 19.2-44 (cont)

Attachment to RAI 19.2-44 c)

VERIFICATION OF ANSYS SOLID65 ELEMENT

A1. Solid65 Element Description

SOLID65 is used for the 3-D modeling of solids with or without reinforcing bars . The solid is capable of cracking in tension and crushing in compression. In concrete applications, the solid capability of the element may be used to model the concrete while the rebar capability is available for modeling reinforcement behaviour.

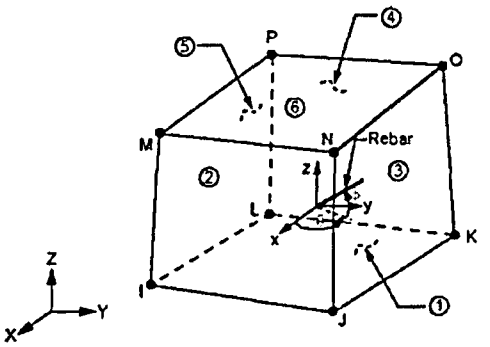

Figure Att. 19.2-44(1) ANSYS Solid65 element geometry

A2. References

For the verification of the ANSYS Solid65 element, two reference has been used.

1. ANACAP-U Validation test. Problem 5.3 Test Report-Two way R/C Slab.
2. ABAQUS Example Problems Manual 1.15 Collapse of a concrete slab. In this example, two ABAQUS products results are compared; ABAQUS/Standard Results and ABAQUS/Explicit Results.

Both of the references compare results on the same problem (same material properties, same geometry and same load case); the two-way supported slab experimentally tested by McNeice (McNeice, A. M., "Elastic-Plastic Bending of Plates and Slabs by the Finite Element Method," Ph. D. Thesis, London University, 1967).

A3. McNeice's Test

The two-way corner-supported slab was experimentally tested by McNeice (1967) and numerically analyzed by many researchers. The 36"x36"x1.75" slab is istropically reinforced at 1.31" from the top surface. Smeared two-way reinforcement is located 1/4 of its depth from the bottom face with a volume ratio steel to concrete of 8.5E-3 in each direction. The slab is loaded at the center and supported at the corners in the transverse (out-of-plane) direction. Some of the concrete material properties required for the analysis were not provided by McNeice, so assumed values are adopted.

A4. Compared data

A double ANSYS results comparison has been carried out:

- Using information provided in ANACAP-U Validation test. 5.3, whose control point is 3" from center of the slab.
- Using information provided in ABAQUS Example Problems Manual 1.15, whose control point is in the middle of the slab.

Since the check-reference for all the calculations (ABAQUS/Standard, ABAQUS/Explicit and ABAQUS/ANACAP-U) is the McNeice's test, the graphs resulting from ANSYS calculations (load vs displacement) are compared also with those from McNeice Test (See Att Figures 19.2-44(4) and (5)). Therefore, the reference data are the experimental McNeice results.

A5. FEM Model

One-quarter model is used with symmetry boundary conditions applied at center lines .

Two mesh sizes, 8x8x3 and 16x16x3, are considered. Figures 19.2-44(2) and 19.2-44(3) show the 8x8x3 mesh.

A6. Material properties

Gilbert and Warner (1978) provide the following properties for the McNeice Slab also adopted in the references.

Concrete	
Elastic modulus	28.6GPa (4150ksi)
Poisson's ratio	0.15
Uniaxial crushing stress	37.92MPa (5.5ksi)
Uniaxial tensile cracking stress	3.17MPa (0.46ksi)
Ratio of biaxial to uniaxial compression failure stress (assumed)	1.2
Density (assumed)	2400kg/m^3 (2.246E-04 lb.s^2/in^4)
Steel reinforcement bars	
Elastic modulus	200GPa (29000ksi)
Yield stress	345MPa (50000ksi)
Density	7800kg/m^3 (7.3E-04 lb.s^2/in^4)

Table Att. 19.2-44(1)

In R/C elements amount of steel reinforcement is input by means of volume ratio of steel in the element to the total volume of the element. Reinforcement is located in a 7.30mm depth layer, so nominal volume ratio must be scaled to depth of the layer.

A7. Results

Figure Att.19.2-44(4) shows the load-deflection curve at the centre of the McNeice slab and the ANSYS results for both 8x8x3 and 16x16x3 mesh models. A very good agreement is reached with the 16x16x3 mesh. The 8x8x3 mesh over-predicts the stiffness of the test model.

Figure Att. 19.2-44(5) shows the load-deflection curve at a 3" offset along symmetry axe from origin of the McNeice slab and the ANSYS results for 16x16x3 mesh model. Also a very good agreement is observed.

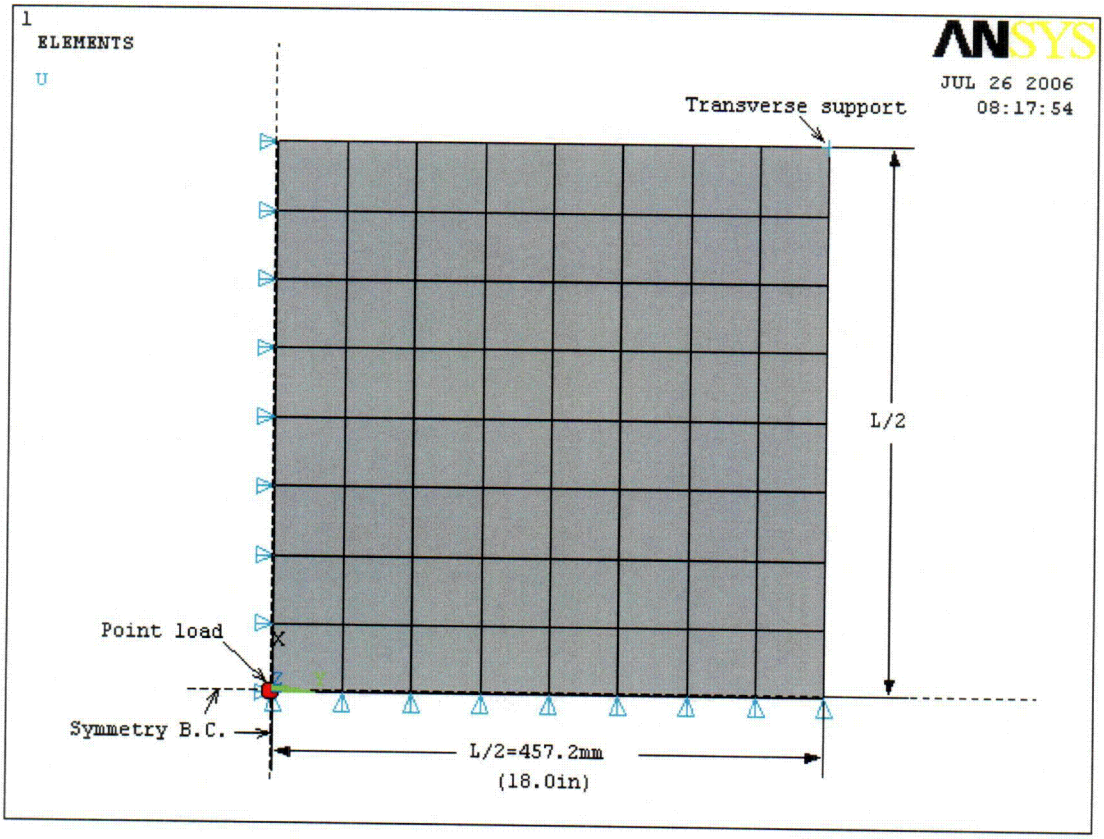

Figure Att. 19.2-44(2) McNeice slab

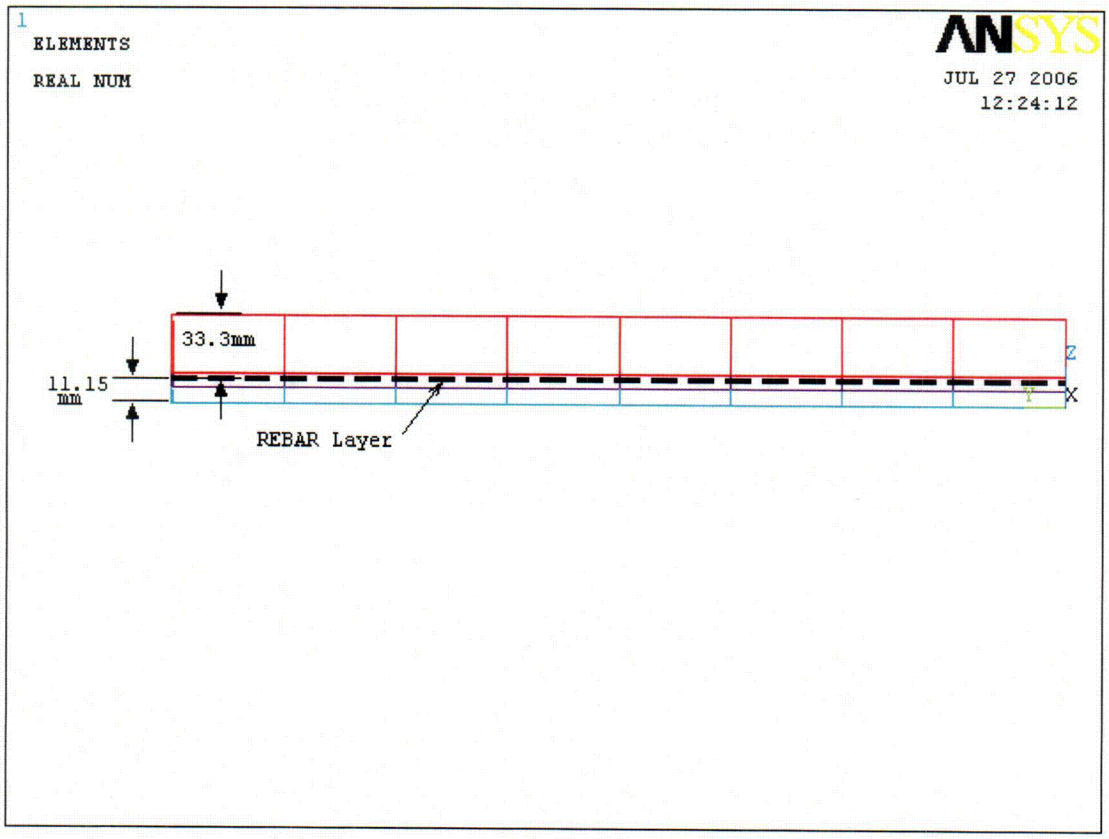

Figure Att. 19.2-44(3) Reinforcement steel layout

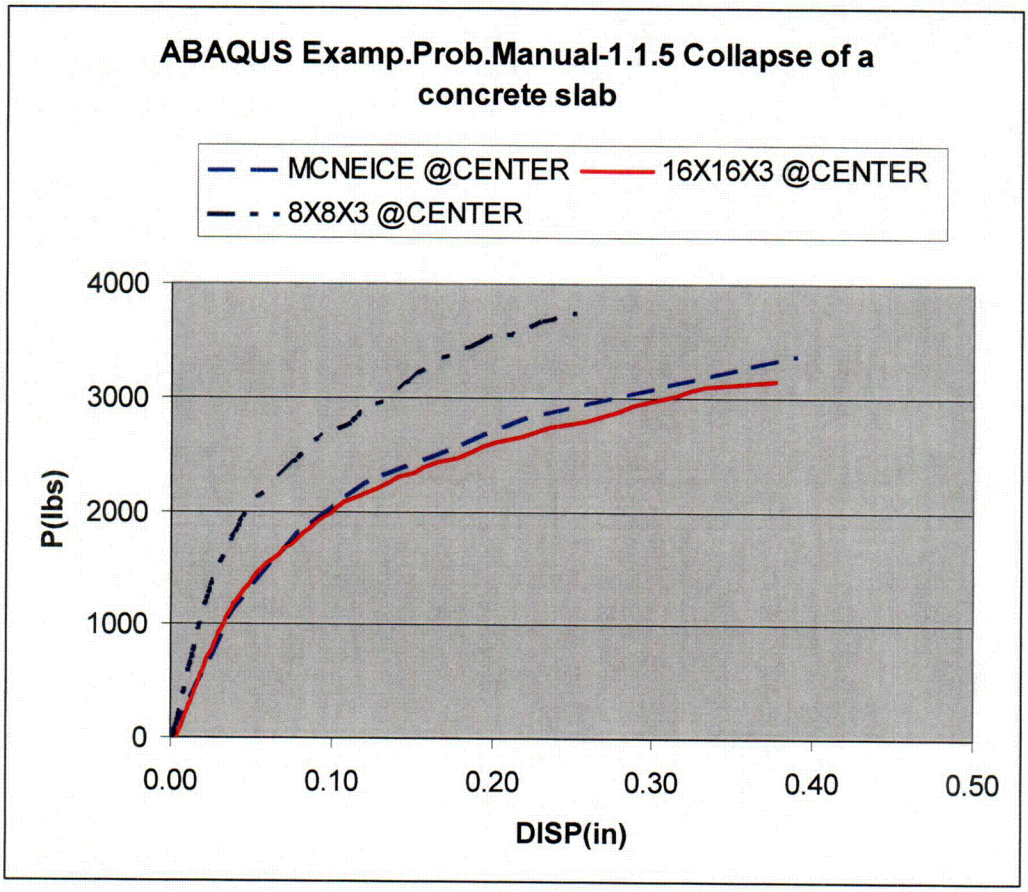

Figure Att. 19.2-44(4) Comparison ANSYS results vs McNeice results (dahsed and blue) at center point

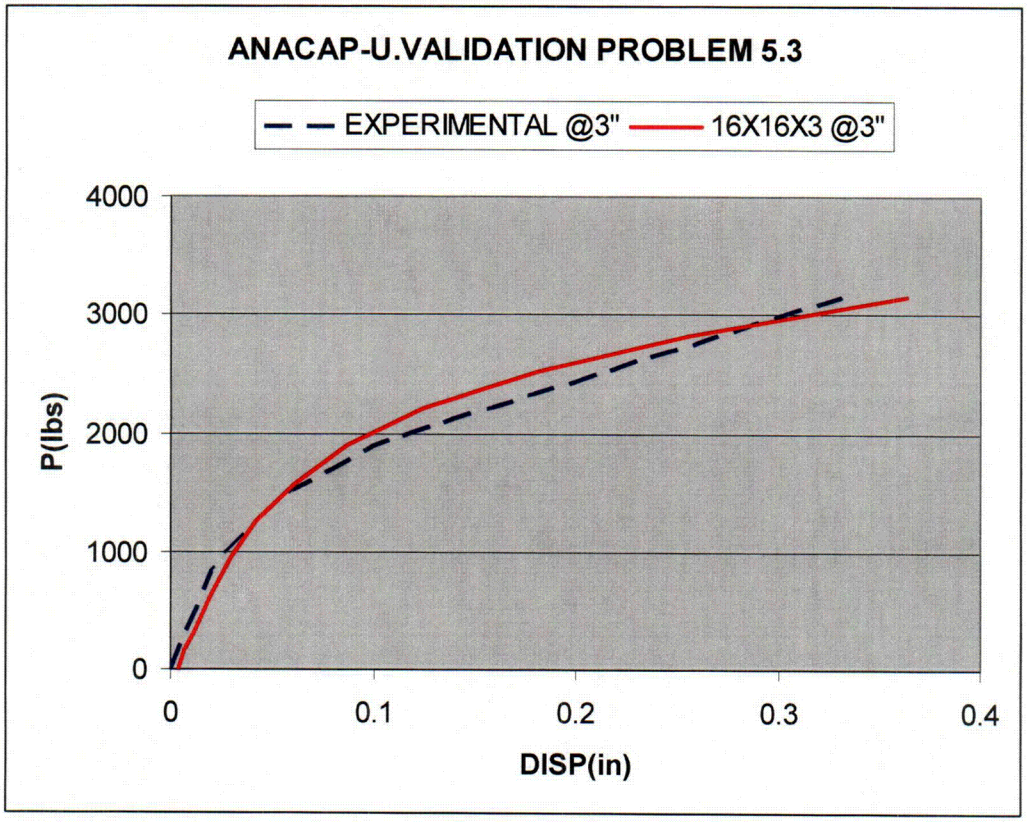

Figure Att. 19.2-44(5). Comparison ANSYS results (solid and red) vs McNeice results (dashed and blue) at 3" offset

NRC RAI 19.2-45

In PRA Revision 1, Appendix B.8.1, GE provides the result of a nonlinear ANSYS analysis for RCCV under internal pressurization and dead load. Four load cases were presented, including the design pressure, integrity test pressure, and two severe accident pressures. Provide the following information:

a) In Appendix B.8, GE stated "The analysis results show that the liner strains are much smaller than the ASME code allowable for factory load category when the internal pressure is as high as 1.468 MPa." (213 psi). Provide the numerical ASME allowable liner strain referred to here.

b) It appears that for load cases SA-1 and SA-2, GE defines the allowable using the ultimate failure strength (F_u for steels and f'_c for concrete). Explain the source for the "code allowable limits", including applicable ASME Service Level, the Code section, and the Code acceptance criteria for rebar, liner plate and concrete (factor times yield stress for steel? Factor times f'_c for concrete?).

c) Explain why in Table B.8-1 of the PRA report, Revision 1, the max. rebar stresses under the 2nd column heading do not match the max. rebar stresses under the component rebar stresses heading, and identify the components and locations where the max. rebar stresses under the 2nd column heading are taken from.

d) Provide the max. rebar strains (including locations) at each pressure level for all components in Table B.8-1, and provide a discussion of comparisons of max. rebar strains with the max. liner strains listed in Table 8.1-1.

e) Explain the response changes from design pressure (PD) to Structural Integrity Test 1 pressure (IT), considering IT = 1.15xPD; ratios of IT/PD responses vary from 0.63 to 1.67.

f) What is the radius at the location of the reported "Max. Radial Defl. Wetwell", and what are the calculated strains at this location (i.e., radial deflection divided by radius)? Compare to the rebar strains.

GE Response

a) The ASME allowables for liner strain, rebar strain and concrete stress under various pressure levels considered are summarized in the following Table 19.2-45 (1). They are compared with the criteria for ultimate pressure capacity.

b) For loads case SA-1 and SA-2 in Table B.8-1, the allowable values in the first row of Table 19.2-45(1) were used. For Level C pressure, the allowable values of Factored Level were based on. For design pressure, the allowable values of Service Level, the third row of Table 19.2-45(1) were used.

c) In Table B.8-1 of the PRA report, Revision 1, some of the maximum rebar stresses under the 2nd column belong to elements of the ANSYS model outside the containment boundary. (As shown in PRA Figure B.8-1, the axisymmetric ANSYS model also accounts for external elements to the containment). For the sake of clarity, PRA Table B.8-1 should be focused on the containment. These data and others in PRA Table B.8-1 will be revised in the next update, as noted in the attached markups.

d) Table 19.2-45(2) and 19.2-45(3) show the maximum rebar strain at each pressure level for all components in Table B.8-1. as well as their locations. See response to RAI 6.2-95 for a detailed comparison of rebar strains and liner strains at 1.468 MPa.

e) Ratios of IT/PD responses varying from 0.63 to 1.67 for a pressure loading ratio of 1.15 are considered reasonable in view of the cracked concrete behavior (not linear). Rebars in cracked zones have higher stresses and strains than those in non-cracked zones, causing local ratios ranging from approximately 0.63 to 1.67. However, the median of the local ratios matches reasonably well the 1.15 ratio.

f) The reported Max. Radial Deflection, is the maximum radial displacement in any point of the containment. In this case it is measured in the middle of the wetwell and is 13.02 mm. For a 18,000 mm inside radius of the containment, radial strain is 0.072%. Radial strain for the rebars in the same location is 0.017% (point 50 in Figure 19.2-45(1)) which is the same order.

	Criteria	Allowable for rebar	Allowable for liner	Allowable concrete stress
SA-2 (P=1.468 MPa)	Ultimate	0.01	0.02	f'_c (34.5 MPa)
(P=1.410 MPa)[1]	Factored Load	$2\varepsilon_y$ (0.004) (ASME CC-3422.1)	0.01 (ASME Table CC-3720-1)	$0.75f'_c$ (25.88 MPa) (ASME Table CC-3421-1)
Maximum Service Level Pressure (P=1.220 MPa)[2]	Service Level	$0.5f_y$ (207 MPa) (ASME CC-3422.1)	0.002 (ASME Table CC-3720-1)	$0.6f'_c$ (20.7 MPa) (ASME Table CC-3431-1)

Notes: (1) Pressure for which the concrete compression is slightly lower than the allowable concrete compression for Factored Loads was used to compare with the Level C pressure for the drywell head. The Level C pressure for drywell head is limiting.
(2) The design pressure is 0.31 MPa. The pressure at which one of the allowables for Service Level is reached is 1.220 MPa.

Table 19.2-45(1). ASME allowables for Various Pressure Levels Compared with the criteria for ultimate pressure capacity

Loading Case.		Component Rebar Strain									
		Mat		SP/S		Wetwell wall		Upper drywell wall		Top Slab	
LC	Load (MPa)	Mer.	Hoop	Mer.	Hoop	Mer.	Hoop	Mer.	Hoop	Mer.	Hoop
DP	0.310	5.010E-06	2.370E-05	1.050E-04	5.090E-05	5.450E-07	3.830E-05	1.040E-04	2.870E-05	9.640E-05	3.710E-05
IT	0.357	2.420E-06	1.640E-05	1.080E-04	5.060E-05	4.920E-05	4.690E-05	1.640E-04	3.590E-05	1.080E-04	4.690E-05
DHUC	1.210	1.125E-03	4.020E-04	8.600E-04	3.520E-04	7.280E-04	5.600E-04	9.440E-04	4.440E-04	9.920E-04	2.050E-04
UC	1.468	1.957E-03	5.970E-04	1.110E-03	4.660E-04	9.260E-04	7.140E-04	1.227E-03	5.880E-04	1.337E-03	2.680E-04

Table 19.2-45(2) rebar strains at each pressure level for all components in PRA Table B.8-1

Loading Case.		Liner		Conc.	Locations										Max. Radial Defl. Wetwell
		Tensile	Comp.		Mat		SP/S		Wetwell wall		Upper Drywell wall		Top Slab		
LC	Load (MPa)	Mer	Hoop		Mer	Hoop	Mer	Hoop	Mer	Hoop	Mer	Hoop	Mer	Hoop	
DP	0.310	#66	#66	#17	#1	#3	#5	#7	#9	#10	#11	#13	#15	#16	#50
IT	0.357	#66	#66	#17	#1	#3	#5	#7	#9	#10	#12	#13	#15	#16	#50
DH	1.210	#66	#66	#18	#2	#4	#6	#8	#9	#10	#12	#13	#14	#16	#50
UC	1.468	#66	#66	#18	#2	#4	#6	#8	#9	#10	#12	#13	#14	#16	#50

Table 19.2-45(3) Locations for all components in PRA Table B.8-1. All numbers are related to Figure 19.2-45(1) and (2)

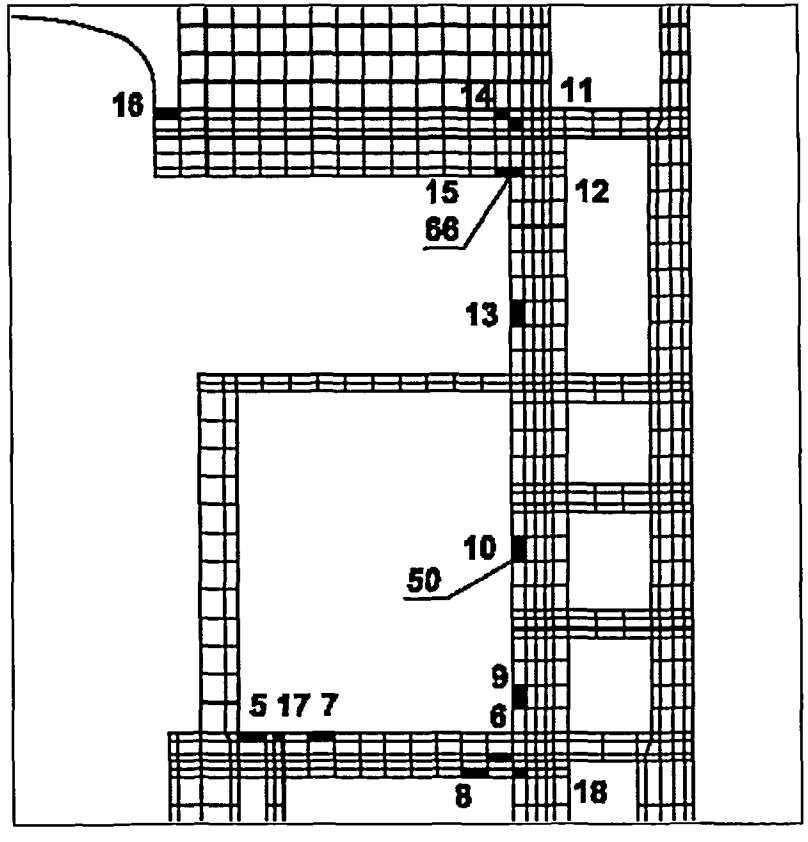

Figure 19.2-45(1) Locations of the data in PRA Table B.8-1 as indicated in Table 19.2-45(3). Upper Drywell and Wetwell.

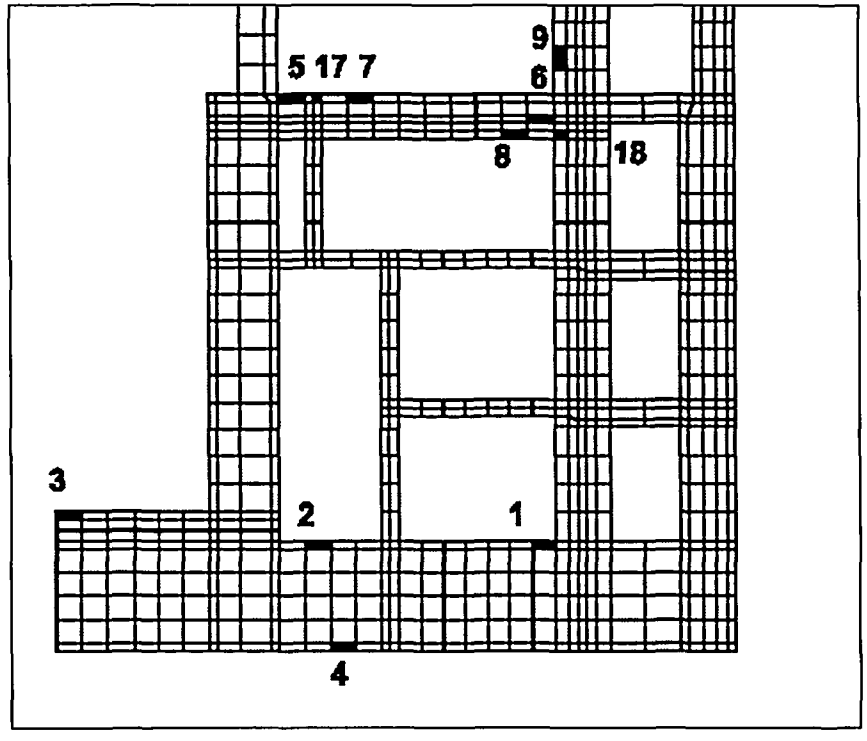

Figure 19.2-45(2) Locations of the data in PRA Table B.8-1 as indicated in Table 19.2-45(3). Lower Drywell and Mat.

NRC RAI 19.2-46

In PRA, Appendix B.8.2.1, GE describes the estimate of the ultimate containment pressure capacity at ambient temperature by extrapolating the ANSYS analysis result to meet a set of failure criteria: rebar at both faces of a cross section reaches yield or concrete fails by shear. Provide the following information:

a) A detailed description of the extrapolation method or analysis and associated data used to arrive at the ultimate component pressure capacities in Table B.8-2 of the PRA report.

b) Detailed data of max rebar stresses (and strains, if available), and strengths of concrete, and liner strains for all components comprising the containment pressure boundary when one component in Table B.8-2 reaches its pressure limit (a table form similar to Table B.8-1 is desirable).

c) Since the concrete failure is characterized as shear failure, describe the shear failure criteria applied.

d) For wetwell and upper drywell, the failure modes are rebar yielding at the DF joint, describe the max strain level in the liner near the DF joint for these failure modes.

GE Response

a) Given the calculated results at ultimate pressure of 1.468 MPa for rebar strain, liner strain for various components of containment as shown in and concrete stress in PRA report Table B.8-2, and given their respective allowable strain/stress limits in Table 19.2-45(1), the extrapolation is done by the following relation:

$$P_{extrap} = \frac{D_{allowable}}{D_{actual}} \cdot P_{UC} \qquad \text{Eq. 19.2-46(1)}$$

Where:

P_{UC}: Ultimate Pressure at room temperature (=1.468 MPa).

$D_{allowable}$: Allowable value of the structural component (allowable strain in rebars, allowable strain in liner or allowable compression stress in concrete).

D_{actual}: Actual calculated data in the structural component (maximum strain in radial, meridian or hoop rebars, maximum strain in liner or maximum compression stress in concrete) at 1.468 MPa pressure and at room temperature.

P_{extrap}: Extrapolated failure pressure at room temperature for rebar, liner or concrete.

Accordingly, the extrapolated failure pressures for rebar, liner and concrete are obtained in each structural element. The minimum failure pressures for each

structural element (wetwell, upper drywell, pedestal, suppression pool slab and basemat) are the values shown in PRA report Table B.8-2, 3rd column.

The values at 500°F (PRA report Table B.8-2, 4th column) are 90% of the ones at room temperature.

b) Detailed data of maximum rebar and concrete stresses for all the components under the pressure that exceeds the pressure limit of 1.468MPa as shown in Table B.8-2 can not be calculated. For illustration purpose the maximum rebar and concrete stresses for various components under the pressure that exceeds the pressure limit were extrapolated as shown below in Table 19.2-46(1). In this table, the only pressure for which the values of liner strains, rebar and concrete stresses are calculated is 1.468 MPa.

Table 19.2-46(1) shows that under the pressures shown in PRA Table B.8-2 greater than the ultimate pressure, most of the rebar stresses go beyond the yield strength and concrete stresses go beyond f'c. However, it is noted that the liner is still well within the Factored Load allowable of 1%.

Load	Maximum Rebar Stress			Liner strain		Concrete	Component rebar tensile stress									
							Mat		SP/S		Wetwell		Upper drywell		Top Slab	
	Pressure Mpa	Merid. Mpa	Hoop Mpa	Tensile mm/mm	Compress. mm/mm	Mpa	Mer.	Hoop	Mer.	Hoop	Mer.	Hoop	Mer.	Hoop	Mer.	Hoop
Calculated values	1.468	284.9	142.9	1.65E-03	-8.59E-04	31.0	284.9	119.5	221.9	93.3	185.3	142.9	245.4	117.5	267.5	53.7
Extrapolated values	2.85	(1)	277.4	3.20E-03	-1.67E-03	(2)	(1)	232.0	(1)	181.1	359.7	277.4	(1)	228.1	(1)	104.3
Extrapolated values	3.63	(1)	353.4	4.08E-03	-2.12E-03	(2)	(1)	295.5	(1)	230.7	(1)	353.4	(1)	290.5	(1)	132.8
Extrapolated values	4.33	(1)	421.5	4.87E-03	-2.53E-03	(2)	(1)	352.5	(1)	275.2	(1)	421.5	(1)	346.6	(1)	158.4
Extrapolated values	4. 8	(1)	(1)	5.40E-03	-2.81E-03	(2)	(1)	390.7	(1)	305.1	(1)	(1)	(1)	384.2	(1)	175.6

Note: (1) Rebar Stresses > 420 MPa (Strain-hardening behavior of steel),

(2) Concrete Stress ~= 35 MPa (f'c=5000psi)

Table 19.2-46(1). Extrapolated values of liner strain, rebar and concrete stress under the theoretical pressures shown in PRA Table B.8-2

c) When concrete element in a section cracks, it is conservatively assumed that the shear reinforcement does not participate to resist shear. As the internal pressure of the containment reaches a certain value such that a concrete section loses its capability to resist shear, the pressure has reached the ultimate capacity of the containment. This pressure is called the ultimate pressure capacity of the containment. In reality, when the concrete element of a section cracks, the shear can still be transferred to the shear reinforcement.

d) Since the results in PRA Table B.8-2 are based on extrapolation, the requested data were not calculated and thus not available. However, according to RAI 6.2-95 Figures 6.2-95(2) thru (4), Table 19.2-46(2) below summarizes the liner and rebar strains near the DF joint at 1.468 MPa at room temperature.

Point	Radial		Mer.		Hoop	
	Shear tie strain	Liner strain	Bar strain	Liner strain	Bar strain	Liner strain
Joint Wetwell/DF (point 58 in Figure 6.2-95(1))	6.89E-04	3.47E-04	8.07E-04	7.92E-04	3.70E-04	3.66E-04
Joint Upper Drywell/DF (point 59 in Figure 6.2-95(1))	-4.97E-04	-6.72E-04	6.74E-04	9.79E-04	5.88E-04	5.91E-04

Table 19.2-46(2) Summary of strains in liner and rebar at 1.468 MPa (room temperature) in DF joint

No DCD changes will be made in response to this RAI.

NRC RAI 19.2-49

In PRA Appendix B.8.2.1.3, GE stated that analytical calculations are carried out to obtain maximum pressure capacity for Passive Containment Cooling System (PCCS) heat exchangers in accordance with Level D limit of ASME Section III, Division 1, Subsection NC, Class 2 Components. Provide a detailed description of these calculations (and associated data) for estimating the ultimate pressure capacity for PCCS heat exchangers at both ambient and 500°F temperatures.

GE Response

The PCCS heat exchanger configuration analyzed is based on the prototype developed for the SBWR project.

Analytical calculations have been performed to establish the maximum pressure that each component of the PCCS heat exchangers can withstand for level D.

The analyses include all the sections up to where the head fitting of the steam line and the head fitting of the drain lines join the RCCV top slab, as well as those sections that have to withstand containment pressure.

The temperature of 500 °F (533 K) is taken into consideration to reduce the allowable stress for materials.

All the sections that have to withstand containment pressure have been considered and verified in accordance with ASME, Section III, Division 1, Subsection NC, Class 2 Components, 2001 Edition.

Stresses for each component are obtained by using the formula applicable for each case and considering the RCCV ultimate pressure value of 1.204 MPa.

The ultimate capacity for each component is determined by comparing the maximum allowable stress for service level D with the stress produced by the RCCV ultimate pressure.

Formulas in NC-3324.3 are used for the calculation of stress in cylindrical shells, that is, for the steam line sleeve, steam line, steam distributor, feed lines, vertical tubes, drain lines, drain line sleeves and headers.

Formulas in NC-3324.9 are used for the calculation of stress in conical shells, that is, for the conical portion of the steam line head fitting and the drain line head fitting.

Formulas in NC-3325 are used for the calculation of stress in flat heads, that is, for the header covers.

Formulas in XI-3223 are used for the calculation of stress in bolts of header covers.

According to Table NC-3321-1, the applicable stress limit is 2·S for service level D, where S is the allowable stress value given in ASME, Section II, Part D, Tables 1A and 3.

The Level D pressure capacity of the most critical component in the PCCS heat exchangers at accident temperature (533 K) is 1.77 MPa, i.e. approximately 1.5 times the containment ultimate pressure (1.204 MPa). The Level D pressure capacity of the most critical component in the PCCS heat exchangers at ambient temperature is higher than 1.77 MPa.

It is concluded that the PCCS heat exchangers have an ultimate capacity higher than that of the RCCV.

No DCD changes will be made in response to this RAI.

NRC RAI 19.2-50

In PRA Appendix B.8.2.2.1, GE described an analysis which scaled the maximum strains in liners from the ANSYS model by a concentration factor of 33, resulting in 3.96% strain at the penetrations, which is much higher than Service Level C limits of ASME Section III, Division 2. GE further stated that this strain level is still far lower than the ultimate fracture strain of 21 percent or the liner material. Provide:

a) a description of the characteristics of the liner material used for the primary containment boundary, including stress-strain relations;

b) justification for using the 21% ultimate fracture strain for the liner material. It should be noted that effective overall liner strain has been limited to 3 percent based on tests performed at Sandia National Labs.

GE Response

a) See response to part e of RAI 19.2-44.

b) The 21% was taken from the SA-516 Gr 70 liner material spec, from ASME II, Part A. As stated in PRA B.8.2.2.1 the "free-field" strain is 0.117% at the capacity pressure of 1.204 MPa. It is much smaller than the limit of 3% effective overall liner strain based on Sandia's tests.

No DCD changes will be made in response to this RAI.

NRC RAI 19.2-57

In PRA, Section 21.3, GE described that the DCH generated superheated gas could induce temperatures in excess of 1000°K in the upper drywell space. It is not clear how the concrete performs under such high temperatures. Provide:

a) a discussion of the duration of concrete exposure to high temperatures, and the depth of thickness of the concrete which will degrade due to exposure to high temperatures.

b) information and a discussion of available test data that supports the GE analysis regarding the concrete performance at high temperatures.

GE Response

a) Calculations were carried out with the MAAP code to determine the long-term temperature history of the upper drywell atmosphere under the assumption that the PCCS and BiMAC systems were functional. We considered a bounding case as found in Section 21 of NEDO-33201 Rev 1 analysis of the DCH event, and we made sure that the starting point of this long-term, systems analysis matched the post-DCH temperature levels found in the DCH event assessment of Section 21 of NEDO-33201 Rev 1. The result is shown in Figure 19.2-57(1). Note as a result of the cooling systems the DCH-induced high temperature spike is just that; in other words it is seen to dissipate in a matter of a few seconds, reaching down to less than 3000 C in ~1 minute. From then on the temperatures decay slowly down to 2000 C in less than 1 hour where it seems to stabilize for the long term (72 hours and beyond).

   We then proceeded to find an upper bound heat up of the concrete by imposing this temperature history on the inner surface of the liner (that is assuming an infinite heat transfer coefficient) along with a gap conductance that was kept conservatively low for the duration of the transient. The results are summarized in Figure 19.2-57(2) and Figure 19.2-57(3). First it is interesting to note that the atmospheric spike attenuates already by the liner, with a peak of only 8000 C. Then we note that the combined effect of slow conduction into the concrete along with the rapid cooling of the atmosphere yields a very slow penetration of a thermal wave whose peak value on the surface is just under 2000 C.

b) We can easily see that the effect of this kind of concrete heating is negligible, both in terms of the amount of material involved as well as in terms of the level of temperatures reached (see Ref 1).

References:

1. "State of the Art Report on High Temperature Concrete Design," DOE/CH/94000-1, Burns and Roe, Oradell, N. J., November 1985.

No DCD changes will be made in response to this RAI.

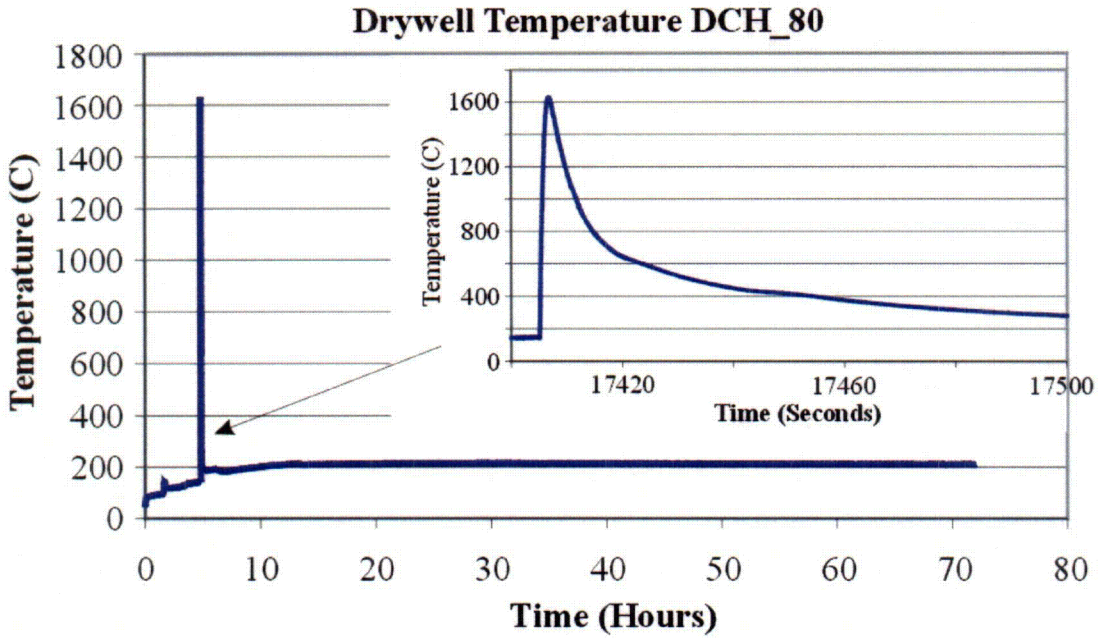

Figure 19.2-57(1). Drywell Temperature History for 80 cm Diameter Breach of RPV

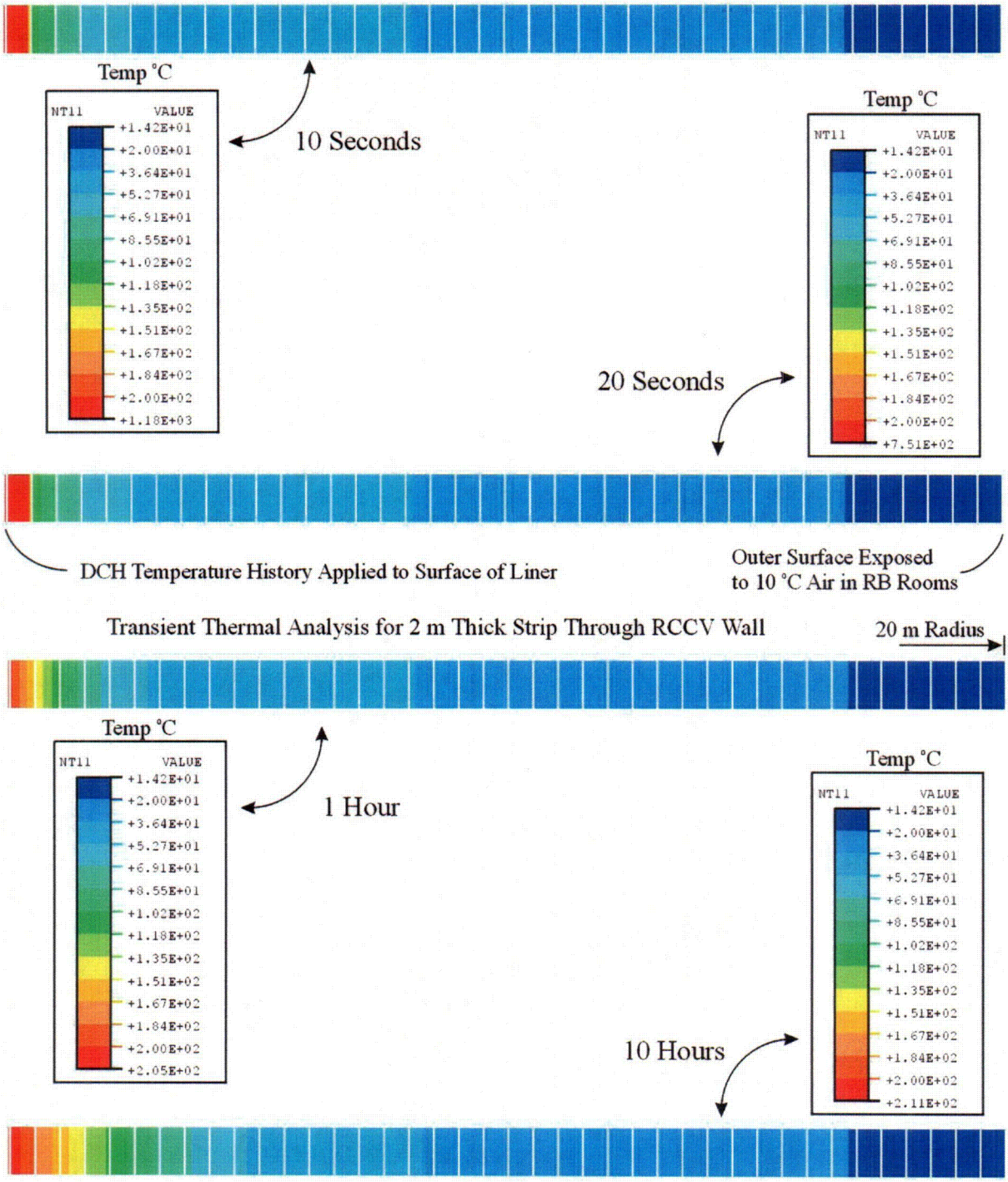

Figure 19.2-57(2). Thermal Contours RCCV Wall under DCH with Large Breach

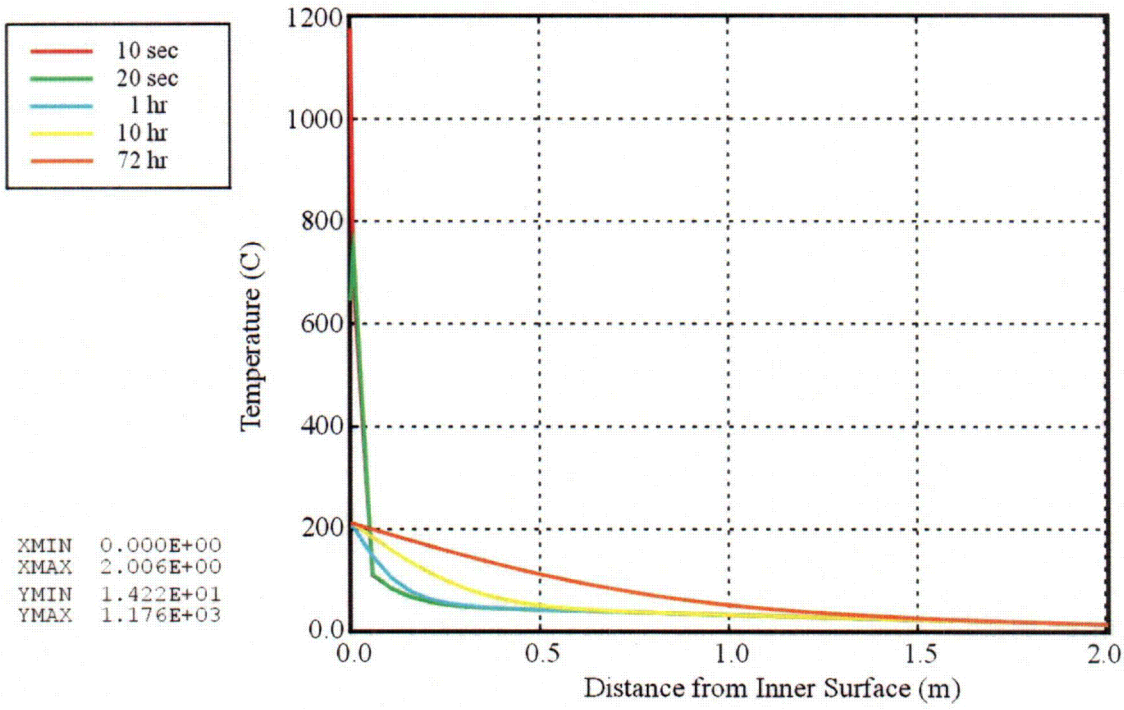

Figure 19.2-57(3). Temperature Profiles in RCCV Wall under DCH with Large Breach

ENCLOSURE 2

MFN 06-268

DCD Section 6.2 and NEDO 33201 Table B.8-1
Markup Pages for
RAIs 6.2-95, & -97, and RAI 19.2-45c

accordance with the statistical analysis performed in the ABWR DCD of the test data on which Eq. 6.2-2 is based, the lower bound and best estimate buckling pressures can be obtained as:

Lower Bound $P_{lb} = 1.5*P_d = 1.975MPa$ (6.2-3)

Best Estimate $P_{be} = 2.27*P_d = 2.989MPa$ (6.2-4)

For Level C evaluation ASME NE-3222 requires a 2.5 factor of safety applied to the best estimate buckling stress. The factor of safety required by Code Case N-284 for Level C is 1.67 and it is applied to the lower bound value. Hence, the Level C internal pressure capability of the drywell head is determined to be the smaller value predicted from the two equations below.

$P_c = P_{be}/2.5 \quad = 1.195MPa \quad$ per NE-3222 (6.2-5)

$P_c = P_{lb}/1.67 \quad = 1.182MPa \quad$ per N-284 (6.2-6)

The most critical of the other RCCV steel penetrations are the main steam pipe penetrations. They have the biggest flued head and anchor sleeves. Considering the loads transmitted by the main steam pipes, the maximum Level C pressure capability can be up to 3.377 MPa. Concerning the other steel penetrations, they have higher Level C pressure capability.

The Level C pressure capabilities of the steel components of major penetrations are summarized in Table 6.2-46. The governing pressure is 1.182 MPa, which is controlled by factor of safety = 1.67 to prevent the drywell head from buckling based on Level C category of loads per Code Case 284.

The PCCS heat exchangers are also part of containment boundary. The Level C pressure capacity of the most critical component in the PCCS heat exchangers is found to be 1.33 MPa.

Level C pressure capability of the concrete containment is evaluated to meet the liner strain limits stipulated in ASME Section III, Division 2, CC-3720. A nonlinear finite element analysis of the containment concrete structure including liner plates is performed for over-pressurization. The analysis results show that when the internal pressure reaches as high as 1.468 MPa, the maximum liner strain is only 0.165% tension, which is well within the 0.3% limit for Factored Load Category specified in ASME Table CC-3720-1. Thus, Level C pressure capacity of the concrete containment is at least 1.468 MPa and it is higher than the 1.182 MPa controlling pressure for the steel components. Demonstration of Level C structural integrity for concrete containments as required by RG 1.7 Revision 3 is to meet CC-3720 requirements which are for liners only. Meeting factored load allowables for concrete and rebar is not a requirement for Level C pressure capability of concrete containments.

In summary, the Level C pressure capability of the ESBWR containment structure is 1.182 MPa under pressure and dead load alone.

6.2.5.5 Post Accident Radiolytic Oxygen Generation

For a design basis loss of coolant accident (LOCA) in the ESBWR, the Automatic Depressurization System (ADS) would depressurize the reactor vessel and the Gravity Driven Cooling System (GDCS) would provide gravity driven flow into the vessel for emergency core cooling. The safety analyses show that the core does not uncover during this event and as a result, there is no fuel damage or fuel clad-coolant interaction that would result in the release of fission products or hydrogen. Thus, for design basis LOCA, the generation of post accident

Table 6.2-46

Level C Pressure Capability of Containment Steel Components

Component	Part	Inner Radius (mm)	Thickness (mm)	Calculated Pressure Capability (MPa gauge)
Drywell Head	Sleeve	5200	50	2.504
	Torispherical head	9407	40	1.182
Equipment Hatch	Sleeve	1200	16	3.465
	Head	2400	20	4.359
Personnel Airlock	Sleeve	1200	16	3.465
Wetwell Hatch	Sleeve	1000	16	4.152
	Head	2000	20	5.229
Main Steam Penetration	Sleeve	1219	50	3.377
	Head	1219	160	3.797

Table B.8-1

Summary of Stresses and Strains

Loading Case		Maximum rebar Stress/Allow. Stress		Liner Strain		Concrete Compress. Stress/ Allowable stress	Component Rebar Tensile Stresses / Allowable Stresses (MPa)										Max. Radial Defl. Wetwell. mm
							MAT		SP/S		Wetwell wall		Upper drywell wall		Top Slab		
Title	P.D. MPa	Merid. MPa	Hoop MPa	Tensile mm/mm	Compress. mm/mm	(MPa)	Mer.	Hoop.	Mer.	Hoop.	Mer.	Hoop.	Mer.	Hoop.	Mer.	Hoop.	
PD	0.310	21.0	10.2	2.40E-04	-1.03E-04	-4.7	1.0	4.7	21.0	10.2	0.1	7.7	20.8	5.7	19.3	7.4	0.68
		207.0	207.0			-20.7	207.0	207.0	207.0	207.0	207.0	207.0	207.0	207.0	207.0	207.0	
IT	0.357	27.8	10.2	2.42E-04	-1.113E-04	-4.8	0.7	3.9	21.4	10.2	9.9	8.7	27.8	6.6	20.6	8.6	0.79
		207.0	207.0			-20.7	207.0	207.0	207.0	207.0	207.0	207.0	207.0	207.0	207.0	207.0	
SA-1	1.210	217.1	119.8	1.17E-03	-5.10E-04	-19.7	217.1	80.4	172.1	70.4	145.6	111.9	188.8	88.7	198.4	41.0	10.19
		429.0	429.0			-34.5	429.0	429.0	429.0	429.0	429.0	429.0	429.0	429.0	429.0	429.0	
SA-2	1.468	284.9	142.9	1.65E-03	-8.59E-04	-31.0	284.9	119.5	221.9	93.3	185.3	142.9	245.4	117.5	267.5	53.7	13.02
		429.0	429.0			-34.5	429.0	429.0	429.0	429.0	429.0	429.0	429.0	429.0	429.0	429.0	